Processing of transparent glass-ceramics by nanocrystallisation of LaF$_3$

N. Hémono, G. Pierre, F. Muñoz, A. de Pablos-Martín, M.J. Pascual *, A. Durán

Instituto de Cerámica y Vidrio (CSIC), C/Kelsen 5, Campus de Cantoblanco, 28049 Madrid, Spain

Abstract

Transparent glass-ceramics have been prepared by heat-treating oxyfluoride glasses in the Na$_2$O–Al$_2$O$_3$–SiO$_2$–LaF$_3$ system. The nanocrystallisation of LaF$_3$ was achieved by controlling time and temperature parameters. Glasses and glass-ceramics were characterised by dilatometry, DTA, XRD and TEM. The mean crystal size (<20 nm) and the crystal fraction increase with the temperature of heat treatment, while they reach a maximum at about 20 h at a temperature close to T_g. The crystallisation of phases containing glass modifier elements as well as F anions leads to the increase in the viscosity of the remaining glass matrix. Phase separation occurs in glass-ceramics depending on the glass composition which affects nanocrystallisation.
© 2009 Elsevier Ltd. All rights reserved.

1. Introduction

Fluoride crystals and glasses are characterised by low phonon energy, optical transparency and rare-earth ion solubility that make them suitable for optical amplifiers and up-conversion devices and lasers.[1–4] However, fluoride crystals are costly to produce and fluoride glasses are characterised by poor chemical durability and mechanical stability. In transparent oxyfluoride glass-ceramics the optical active ion may be incorporated into a fluoride crystalline phase, thus offering a better alternative to both fluoride glasses and crystals.[5]

Wang and Ohwaki reported the first transparent PbF$_2$-containing oxyfluoride glass-ceramic obtained by heat treatment.[6] Dejneka reported LaF$_3$-containing glass-ceramics as a more suitable host for rare-earth ions (RE) due to the better solubility of LaF$_3$ for RE than PbF$_2$.[7] A large concentration of nanocrystals with narrow size distribution is required in order to minimize the scattering losses in photonic applications, which can be done by controlling the nucleation and crystal growth within the glass matrix. The crystallisation studies are usually focused on isochemical systems, in which both crystals and glass matrix have the same composition that is not the case in Na$_2$O–Al$_2$O$_3$–SiO$_2$–LaF$_3$ system, where only

LaF$_3$ will crystallise. Rüssel explained the nanocrystallisation of CaF$_2$ in silicate glasses through the increase in the viscosity of the remaining glass matrix.[8] The crystal–glass interface acts as a diffusional barrier and notably decelerates the crystal growth velocity that leads to the crystallisation of nanocrystals with size in the range from 10 nm to 50 nm. The crystallisation behaviour, structure and the fluorescence properties of Na$_2$O–Al$_2$O$_3$–SiO$_2$–LaF$_3$ and Er^{3+} and Yb^{3+}-doped glass-ceramics have already been investigated[9–17] but the nucleation-crystal growth process and the variation on the size and number of crystals as a function of the thermal treatment as well as the interface characteristics need to be studied. The present work is based on this objective and constitutes a preliminary study on the processing and characterisation of transparent LaF$_3$-containing glass-ceramics. Glasses and glass-ceramics have been characterised by dilatometry, differential thermal analysis, X-ray powder diffraction and transmission electron microscopy in order to determine the influence of the composition and the time–temperature conditions on the size and the quantity of nanocrystals.

2. Experimental

2.1. Processing of glass-ceramics

The oxyfluoride glasses were prepared by melting reagent grade SiO$_2$ (Saint Gobain, 99.6%), Al(OH)$_3$ (Aldrich) or Al$_2$O$_3$

* Corresponding author.
 E-mail address: mpascual@icv.csic.es (M.J. Pascual).

Table 1
Nominal and analysed compositions (in mol%), glass transition temperatures (T_g) and the temperature of the maximum of the crystallisation peak (T_c) of the three transparent oxyfluoride glasses.

	40Si–12La		40Si–10La		55Si–10La	
	Nominal	Analysed	Nominal	Analysed	Nominal	Analysed
SiO_2	40	45.5	40	39.3	55	56.4
Al_2O_3	30	25.7	30	33.0	20	19.8
Na_2O	18	16.5	20	18.2	15	13.6
LaF_3	12	7.5	10	6.6	10	7.8
La_2O_3	0	4.8	0	2.9	0	2.4
F^- (wt%)	7.7	4.6	6.6	4.1	6.9	5.2
T_g (°C) ± 2 °C	570	583	598			
T_c (°C) ± 2 °C	685	875	706			

(Panreac), Na_2CO_3 (Panreac, 99.5%) and LaF_3 (Panreac, 99%) in an electric furnace. The batches were first calcined in covered platinum crucibles up to 1300–1400 °C and then melted 2 h within the temperature range of 1450–1600 °C depending on composition. The melts were quenched in air onto a brass mould and then annealed above the glass transition temperature. Glass-ceramics were obtained by controlled crystallisation of LaF_3 by using cubic samples that were heat treated at temperatures between T_g and $T_g + 100$ °C in steps of 20 or 25 °C during 20 h. Kinetics studies were also performed in order to determine the influence of the treatment time at temperature close to T_g (from 10 h up to 72 h).

2.2. Characterisation of glasses

The base glass compositions were chemically analysed by X-ray fluorescence and flame photometry.

Glass transition temperature (T_g) was determined by dilatometry in a Netzsch Gerätebau dilatometer, model 402 EP, using a 2 °C min^{-1} heating rate in air. The estimated error on T_g is ±2 °C. Differential thermal analysis (DTA) was performed on a Netzsch HSTA 409 with a heating rate of 10 °C min^{-1} in air and a particle size range of 500–800 μm.

Oxyfluoride glasses and glass-ceramics were characterised by transmission electron microscopy (TEM) in a Hitachi H7100 employing the carbon replica method. The samples were chemically etched with a 5% HF solution during 20 s.

Powder XRD analyses were carried out with a D-5000 Siemens diffractometer using monochromatic Cu Kα radiation (1.5418 Å). After checking the crystallisation of LaF_3, the angular range 22–30° (2θ) with a step length of 0.03° (2θ) and a fixed counting time of 12 s/step was chosen to record the LaF_3 (1 1 1) peak in optimum conditions in order to minimize the errors in the mean crystal size calculation.

3. Results

Table 1 summarises the nominal and analysed compositions (in mol%), glass transition temperatures and the temperature of the maximum of the crystallisation peak of the three oxyfluoride glasses belonging to the system $Na_2O–Al_2O_3–SiO_2–LaF_3$ studied in the present work. Chemical analysis of glass 40Si–12La demonstrates that the maximum incorporation of fluorine into

the glass matrix, as expected in silicate glasses, is less than 5 wt%, which corresponds to 10 mol% of LaF_3 in the nominal composition. The LaF_3 content has been fixed at 10 mol% for the other two glasses in order to avoid a big excess of La_2O_3 in the glass matrix after fluorine volatilisation. The use of aluminium hydroxide for glass 40Si–12La leads to a large difference between nominal and analysed compositions, which may be due to the highly hydrated $Al(OH)_3$. The other two glasses were obtained using Al_2O_3, calcined at 800 °C during 12 h, in order to optimize the agreement of Al_2O_3 content between nominal and analysed compositions.

Thermal treatments up to $T_g + 100$ °C of oxyfluoride glasses 40Si–12La and 55Si–10La showed crystallisation of LaF_3 only, while it was not possible for glass 40Si–10La. Whereas the oxyfluoride glass-ceramics remain transparent in the case of glass 40Si–12La, the samples become translucent for heat treatment from 640 °C in the case of glass 55Si–10La.

Fig. 1 depicts the XRD pattern of glasses 55Si–10La treated 20 h at 620 °C, 40Si–12La treated 20 h at 645 °C and 40Si–10La treated at 680 °C during 20 h. The XRD patterns of the two first glass-ceramics match that of hexagonal LaF_3 (PDF file No. 32-0483) whereas 40Si–10La glass-ceramic matches that of LaF_3, cristobalite (PDF file No. 75-1544) and an unknown phase. High alumina content (33 mol%) might inhibit the crystallisation of single LaF_3 phase at temperatures below crystallisation of cristobalite.

Figs. 2 and 3 display the XRD patterns, scanned over the angular range of 22–30° (2θ), of the glass-ceramics obtained
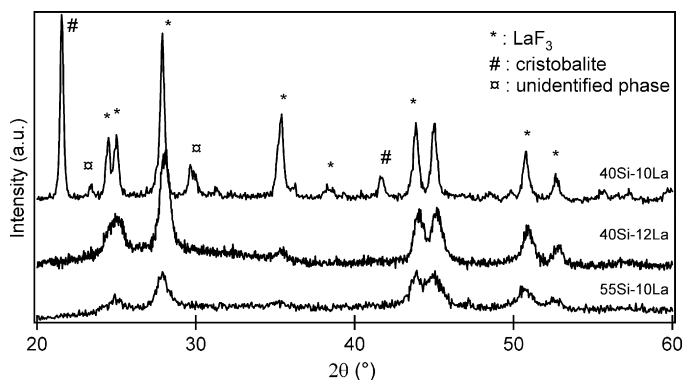

Fig. 1. XRD patterns of glasses 55Si–10La treated 20 h at 620 °C, 40Si–12La treated 20 h at 645 °C and 40Si–10La treated 20 h at 680 °C.
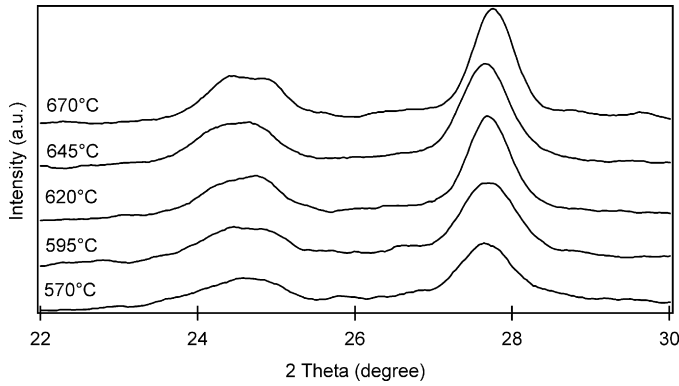
Fig. 2. XRD pattern of glass 40Si–12La treated 20 h from 570 °C (T_g) up to 670 °C.
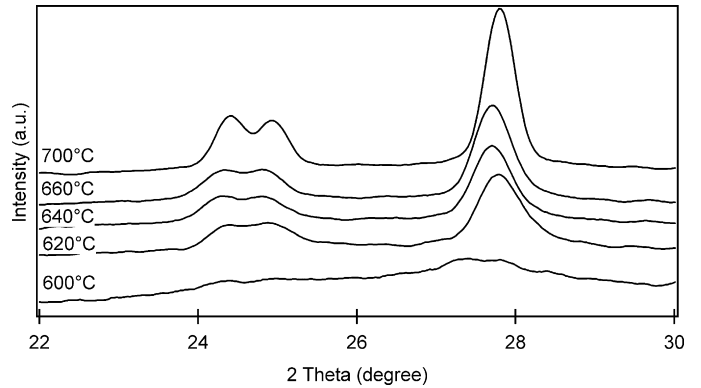

Fig. 3. XRD pattern of glass 55Si–10La treated 20 h from 600 °C (T_g) up to 700 °C.

by heat treatment at temperatures from T_g up to $T_g + 100\,°C$ during 20 h. In both cases, the intensity of the diffraction peaks increases with the temperature of heat treatment, which is related to an increase in the crystal fraction. The XRD lines were fitted by curves of Gaussian shape. The size of the crystals has been calculated using the Scherrer equation on the $2\theta \approx 27.5°$ peak of LaF$_3$ (1 1 1) from the patterns scanned over the angular range 22–30° (2θ) with a step length of 0.03° (2θ) and a fixed counting time of 12 s/step following equation:

$$D = \frac{G\lambda}{B \cos \theta} \tag{1}$$

where D is the mean crystal size, G is a constant whose value is 0.9, λ the wavelength of X-rays, B the corrected full width at half maximum of the peak and θ the Bragg angle. The area under the $2\theta \approx 27.5°$ peak was also calculated to evaluate the trends in the crystal fraction which is proportional to the area under the peak. The errors for size and areas are given by the peak fit determination.

Fig. 4a depicts the variation of the mean crystal size as a function of time for glasses 40Si–12La and 55Si–10La treated at 570 °C (T_g) and 620 °C ($T_g + 20\,°C$), respectively. Both glass-ceramics show an increase in the mean crystal size up to 20 h treatment followed by an asymptotic limit. However, the size of
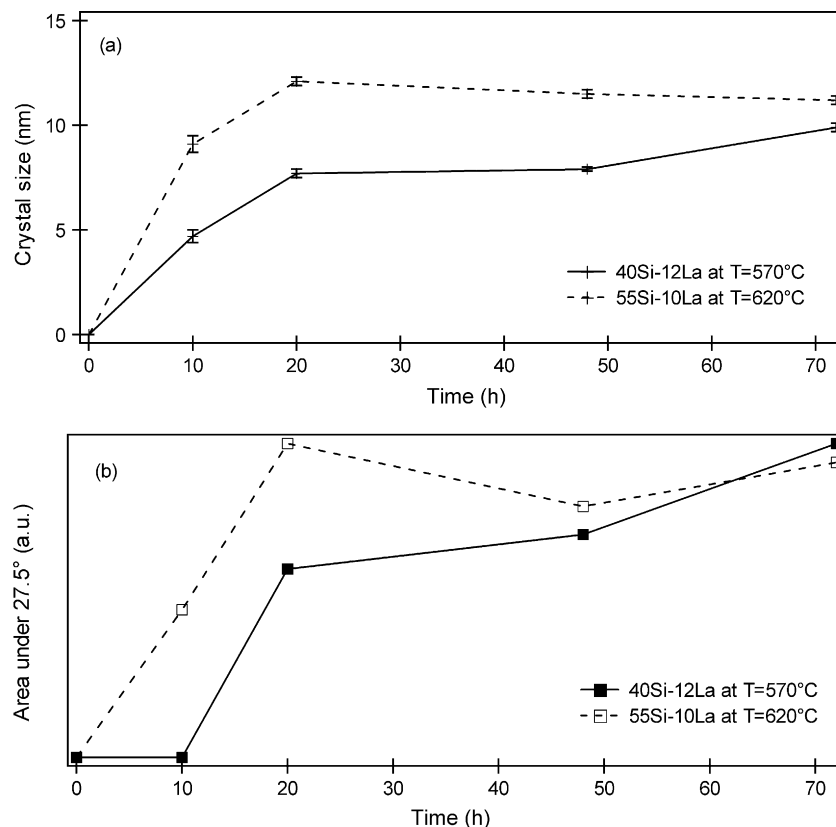

Fig. 4. Variation of the mean crystal size (a) and area under the 27.5° diffraction peak (b) of glass 40Si–12La treated at 570 °C and glass 55Si–10La treated at 620 °C as a function of time of heat treatment. The lines are drawn as a guide to the eyes.
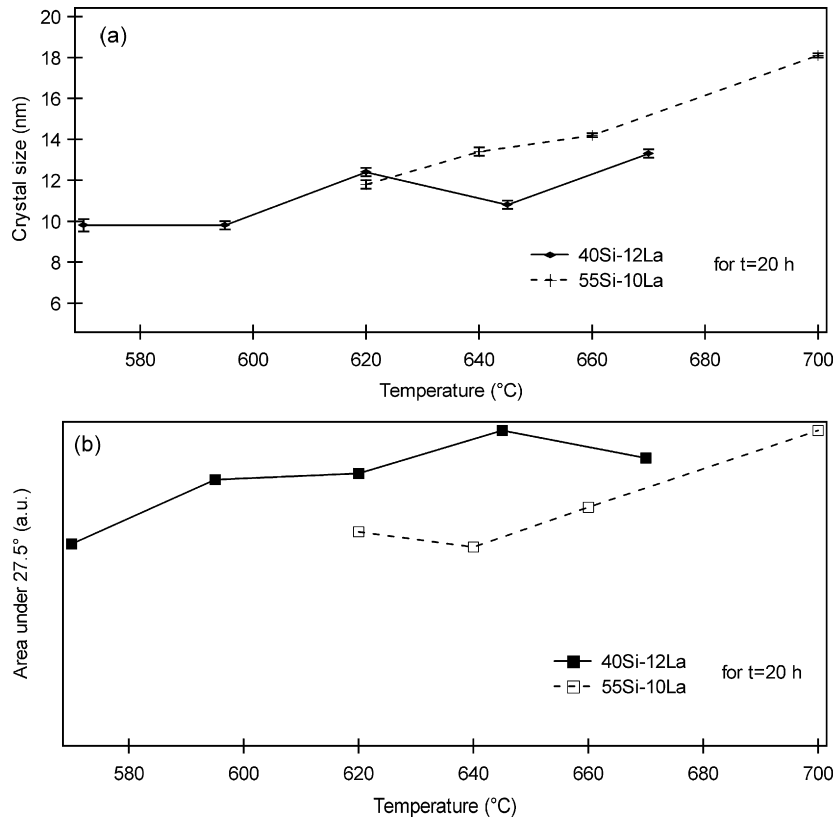
Fig. 5. Variation of the mean crystal size (a) and area under the 27.5° diffraction peak (b) of glasses 40Si–12La and 55Si–10La treated during 20 h as a function of the temperature of heat treatment. The lines are drawn as a guide to the eyes.

the crystals reaches a bigger value for glass 55Si–10La within the whole time interval, being of 11 nm and 9 nm for glasses 55Si–10La and 40Si–12La, respectively.

Fig. 4b displays the variation of the area as a function of time of heat treatment for glass 40Si–12La treated at 570 °C and glass 55Si–10La treated at 620 °C. In both cases, the area increases up to 20 h of treatment while it remains approximately constant for longer treatment times.

Fig. 5a shows the variation of the mean crystal size as a function of temperature for glasses 40Si–12La and 55Si–10La treated during 20 h. For both glasses, the mean crystal size slightly increases with temperature and the maximum size being smaller than 20 nm. Fig. 5b depicts the variation of the area as a function of temperature of heat treatment for glasses 40Si–12La and 55Si–10La treated during 20 h, showing a slight increase within the temperature range studied.

Fig. 6 shows the variation of the glass transition temperature as a function of the treatment temperature of glasses 40Si–12La and 55Si–10La for a constant time of 20 h. In both cases, T_g values are increasing linearly with the temperature of heat treatment while this variation is greater for glass 55Si–10La.

Fig. 7 displays the TEM micrographs of the glass 40Si–12La (a) and its corresponding glass-ceramic obtained at 670 °C during 20 h (b). A droped-like phase separation can be observed in the base glass, which is enhanced after the thermal treatment as it can be seen in the micrograph of the glass-ceramic (Fig. 7b). This phase separation can be the responsible for the formation

of agglomerates of around 100 nm of LaF₃ crystals, at the same time that the nanocrystallisation takes place.

Fig. 8 displays the TEM micrographs of base glass 55Si–10La (a) and the glass-ceramic obtained at 700 °C during 20 h (b). In this case, a slight phase separation phenomenon is also observed but in a much less extent than in case of glass 40Si–12La. Fig. 8b shows a homogeneous distribution of crystals with an estimated size of 20–25 nm, which is in good agreement with the calculation from the XRD pattern (<20 nm). Electron diffraction experiments confirmed the crystallisation of LaF₃ in the two glass-ceramics.
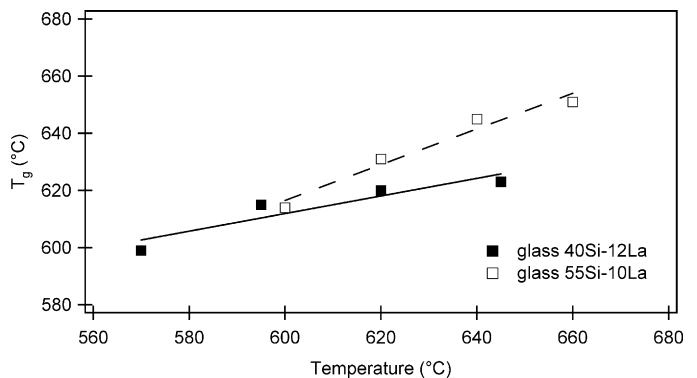

Fig. 6. Variation of the glass transition temperature of glasses 40Si–12La and 55Si–10La as a function of the treatment temperature for a constant time of 20 h.
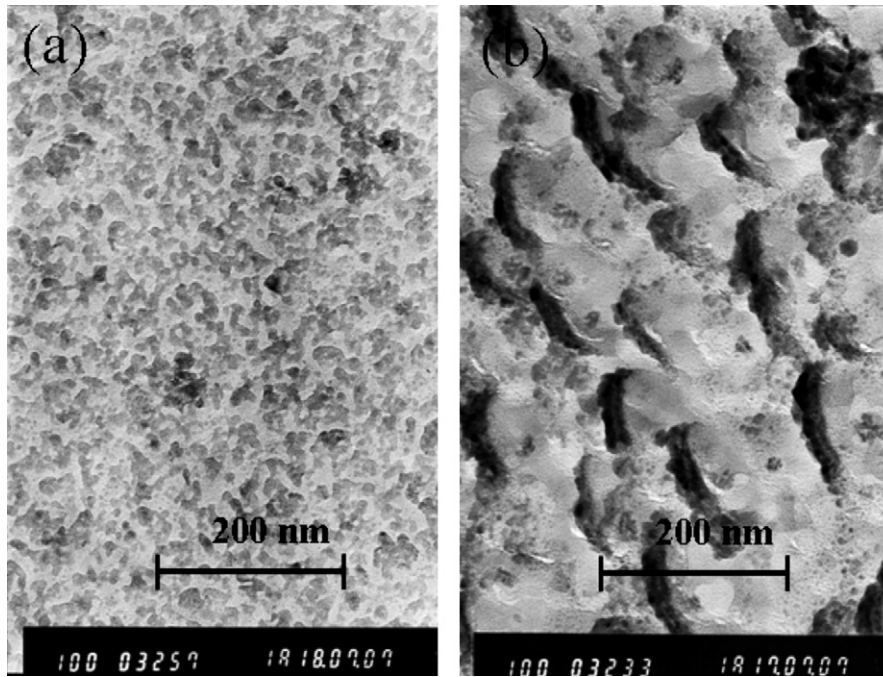
Fig. 7. TEM images of glass 40Si–12La, (a) base glass and (b) glass-ceramic obtained after treatment at 670 °C during 20 h.
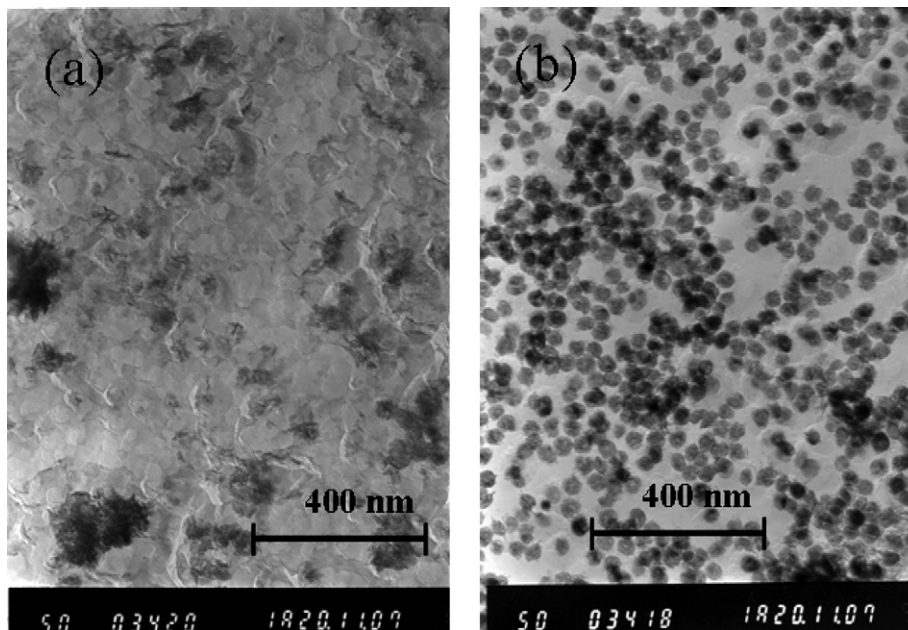

Fig. 8. TEM images of glass 55Si–10La, (a) base glass and (b) glass-ceramic obtained after treatment at 700 °C during 20 h.

4. Discussion

The LaF_3 crystallisation behaviour has been shown to be similar for glasses 40Si–12La and 55Si–10La with regard of the mean crystal size and area. The size and crystalline fraction increase up to 20 h treatment at temperatures just above the glass transition temperature, while they remain approximately constant for longer treatment times. However, the growing in size and crystallisation of LaF_3 is slightly bigger for the composition with higher SiO_2 content (glass 55Si–10La).

The nominal SiO_2/Al_2O_3 ratios are 1.33, 1.33 and 2.75 for the studied glasses 40Si–12La, 40Si–10La and 55Si–10La, respectively. However, chemical analyses show quite different values for glasses 40Si–12La and 40Si–10La, i.e. 1.77 and 1.19, respectively. Glass 40Si–10La showed the smallest tendency for crystallisation of single LaF_3 phase at low temperatures. Thus, it can be assumed in this case, that the smaller the SiO_2/Al_2O_3 ratio, the lower the crystallisation ability. Even though the treatment temperature of glass 55Si–10La was $T_g + 20$ °C in order to be able to calcu-

late the mean crystal size, Fig. 4 shows a bigger size and amount of crystals as a function of time for glass 55Si–10La than for glass 40Si–12La, which is in accordance with the biggest tendency for crystallisation as the SiO_2/Al_2O_3 ratio increases.

On the other hand, crystal size and area slightly increase with treatment temperature for a constant time of 20 h for both glasses. In this case, there seems not to be a limit to the growing of crystals through the viscosity of the crystal–glass interface as in the case of CaF_2-containing glass-ceramics studied by Rüssel.[14] The crystalline fraction is assumed to increase within the temperature range studied at the same time that the mean crystal size increases from 10 to a maximum of 20 nm.

Glass transition temperature increases with treatment temperature for both glasses 40Si–12La and 55Si–10La, according to a decrease in the modifier content within the glass matrix composition after LaF_3 crystallisation. Nevertheless, the slope of the increase is bigger for glass 55Si–10La, which might be influenced at the same time by crystallisation as well as phase separation phenomena. If it only depended on the crystalline size and fraction, one may assume that a bigger crystallisation rate at a fixed temperature will lead to a bigger removal of glass modifiers from the glass matrix, thus giving rise to a more SiO_2 and Al_2O_3 enriched glassy phase with a higher T_g.

The nanocrystallisation behaviour in this system seems to be preceded by a phase separation process as shown in the TEM micrographs. A more completed study at the nanometer level using energy-filtered TEM imaging techniques (zero-loss filtering and elemental mapping) is to be published.[18] In this work, it is revealed that La- and Si-enriched phase-separation droplets are precipitated already during the preparation of initial glass. Upon conversion of the glass in to a nano glass-ceramics by appropriate annealing, LaF_3 nanocrystals are formed within these droplets. Excess silicon, also contained in the phase-separation droplets, is relocated towards the periphery of the droplets allowing only slight crystal growth.

5. Conclusions

Three oxyfluoride glass compositions in the system $Na_2O–Al_2O_3–SiO_2–LaF_3$ have been studied. Fluorine losses cannot be avoided and the maximum incorporation is less than 5 wt% (around 10 mol% of LaF_3). The formation of LaF_3 single phase depends on the glass composition. Nanocrystals (size < 20 nm) have been obtained; the mean crystal size and the crystal fraction increase with the temperature of heat treatment and reach a maximum at about 20 h of treatment at temperature near T_g. Glass transition temperature increases with the temperature of treatment; the crystallisation of LaF_3 leads to a decrease of network modifier in the residual glass matrix. A phase separation occurs in base glasses and glass-ceramics that might affect the nanocrystallisation process.

References

1. Tran, D. C., Sigel Jr., G. H. and Bendow, B., Heavy metal fluoride glasses and fibers: A review. *J. Lightwave Technol.*, 1984, **LT-2**(5), 566–586.
2. Ainslie, B. J., Davey, S. T., Szebesta, D., Williams, J. R., Moore, M. W., Whitley, T. and Wyatt, R., A review of fluoride fibres for optical amplification. *J. Non-Cryst. Solids.*, 1995, **184**, 225–228.
3. Yamada, M., Kanamori, T., Terunuma, Y., Oikawa, K., Shimizu, M., Sudo, S. and Sagawa, K., Fluoride-based erbium-doped fiber amplifier with inherently flat gain spectrum. *IEEE Photon. Technol. Lett.*, 1996, **8**(7), 882–884.
4. Downing, E., Hesselink, L., Ralston, J. and Macfarlane, R., A three-color solid-state, three-dimensional display. *Science*, 1996, **273**, 1185–1189.
5. Auzel, F., Pecile, D. and Morin, D., Rare earth doped vitroceramics: New, efficient, blue and green emitting materials for infrared up-conversion. *J. Electrochem. Soc.*, 1975, **122**, 101–107.
6. Wang, Y. and Ohwaki, J., New transparent vitroceramics codoped with Er^{3+} and Yb^{3+} for efficient frequency upconversion. *Appl. Phys. Lett.*, 1993, **63**(24), 3268–3270.
7. Dejneka, M. J., The luminescence and structure of novel transparent oxyfluoride glass-ceramics. *J. Non-Cryst. Solids*, 1998, **239**, 149–155.
8. Rüssel, C., Nanocrystallization of CaF_2 from $Na_2O/K_2O/CaO/Al_2O_3/SiO_2$ glasses. *Chem. Mater.*, 2005, **17**, 5843–5847.
9. Tanabe, S., Hayashi, H., Hanada, T. and Onodera, N., Fluorescence properties of Er^{3+} ions in glass ceramics containing LaF_3 nanocrystals. *Opt. Mater.*, 2002, **19**, 343–349.
10. Goutaland, F., Jander, P., Brocklesby, W. S. and Dai, G., Crystallisation effects on rare earth dopants in oxyfluoride glass ceramics. *Opt. Mater.*, 2003, **22**, 383–390.
11. Środa, M., Waclawska, I., Stoch, L. and Reben, M., DTA/DSC study of nanocrystallisation in oxyfluoride glasses. *J. Therm. Anal. Cal.*, 2004, **77**, 193–200.
12. Hu, Z., Wang, Y., Bao, F. and Luo, W., Crystallization behavior and microstructure investigations on LaF_3 containing oxyfluoride glass ceramics. *J. Non-Cryst. Solids*, 2005, **351**, 722–728.
13. Ma, E., Hu, Z., Wang, Y. and Bao, F., Influence of structural evolution on fluorescence properties of transparent glass ceramics containing LaF_3 nanocrystals. *J. Lumin.*, 2006, **118**, 131–138.
14. Reben, M., Waclawska, I., Paluszkiewicz, C. and Środa, M., Thermal and structural studies of nanocrystallisation of oxyfluoride glasses. *J. Therm. Anal. Cal.*, 2007, **88**, 285–289.
15. Reben, M., and Waclawska, I., Structure and nanocrystallization of $SiO_2–Al_2O_3–Na_2O–LaF_3$ glasses. *Proceedings of the XXI International Congress on Glass*. Strasbourg, France.
16. Chen, D., Wang, Y., Yu, Y. and Ma, E., Influence of Yb^{3+} content on microstructure and fluorescence of oxyfluoride glass ceramics containing LaF_3 nano-crystals. *Mater. Chem. Phys.*, 2007, **101**, 464–469.
17. Jin, W., Xusheng, Q., Xianping, F. and Minquan, W., Preparation and luminescence of Er^{3+} doped oxyfluoride glass ceramics containing LaF_3 nanocrystals. *J. Rare Earths*, 2006, **24**, 67–71.
18. Bhattacharyya, S., Höche, Th., Hemono, N., Pascual, M. J., and van Aken, P. A., Study of nanocrystallization behavior in $LaF_3/NaO/Al_2O_3/SiO_2$ glass using transmission electron microscopy. *J. Cryst.*, submitted for publication.